

# A MODIFICATION TO PRESTON'S EQUATION AND IMPACT ON PATTERN DENSITY EFFECT MODELING

A. Maury\*, D. Ouma\*\*, D. Boning\*\*, J. Chung\*\*

\*Lucent Technologies Bell Laboratories, Orlando, FL 32819

\*\*Massachusetts Institute of Technology, Cambridge, MA 02139

## ABSTRACT

We have shown that the removal rate of blanket oxide layers does not follow Preston's law strictly. There exist two polishing regimes which are distinguished by the magnitude of the pressure and relative velocity product,  $pv$ . For large  $pv$  typically used for polishing, a constant term should be added to the Preston term for better fit to experimental data. The modified Preston's equation has been incorporated into a closed-form analytic ILD thickness model to obtain a better agreement with experimental observations.

## I. INTRODUCTION

As the use of chemical mechanical polishing (CMP) is extended to more challenging applications such as shallow trench isolation (STI), soft metal damascene, and CMP-only interlevel dielectric (ILD) planarization, more accurate models are required for process optimization. The most basic model for wafer-scale material removal was developed by Preston [1], and in general, good agreement has been observed between Preston's equation and experimental results for blanket oxide polishing. The model remains the standard reference for more detailed models such as the micro-scale fracture model proposed by Cook [2]. In recent years, it has been extended to account for layout pattern density on planarization [3,4].

Despite the success of the model, a close examination of experimental data has revealed that Preston's equation is not satisfied strictly. We have observed that for blanket-wafer oxide polishing, the addition of a constant term to Preston's equation results in a better fit to most experimental results. Apparently there exist two regimes of operation depending on the magnitude of the product of the pressure and relative velocity between the wafer and pad. For large  $pv$  typically used in polishing, the removal rate is linear but with a non-zero intercept. In this work, the modified Preston's equation has also been incorporated into an analytic closed-form ILD thickness model presented in [3] to obtain a better agreement with experimental observations.

This paper is divided into five main sections. In Section II, we review the evaluation of relative velocity between any position on the wafer and the pad since it is important that the correct relative velocity be used in Preston's equation. In Section III, we present the results for TEOS polishing to demonstrate the existence of two polishing regimes depending on the magnitude of  $pv$ . Modification of the analytic ILD thickness model to account for the non-Prestonian effect is detailed in Section IV. Finally, the conclusion is presented in Section V.

## II. PRESTONIAN BEHAVIOR OF REMOVAL RATE

Preston's equation states that the removal rate is proportional to the product of the polish pressure,  $p$ , and relative velocity,  $v$ , i.e.

$$\frac{dz}{dt} = -k_p pv \quad (1)$$

where  $z$  is the film thickness and  $k_p$  is the Preston coefficient. The polish pressure is directly given as the down force while the relative velocity must be obtained from the carrier and table angular velocities (both usually given in rpm). Details of relative velocity calculations are presented in [1] and reviewed here for completeness. Figure 1 shows a typical rotary machine setup.  $O$  is the center of the polish table and  $P$  is the axis of rotation of the wafer carrier. The circle of radius  $R$  centered at  $P$  is a ring of wafer and the goal is to determine the relative velocity at point  $Q$  on the wafer and finally the effective relative velocity at any point on the ring. The carrier usually oscillates along  $OP$  to ensure even pad degradation and improved uniformity. The average offset,  $e$ , will be used in the derivation.

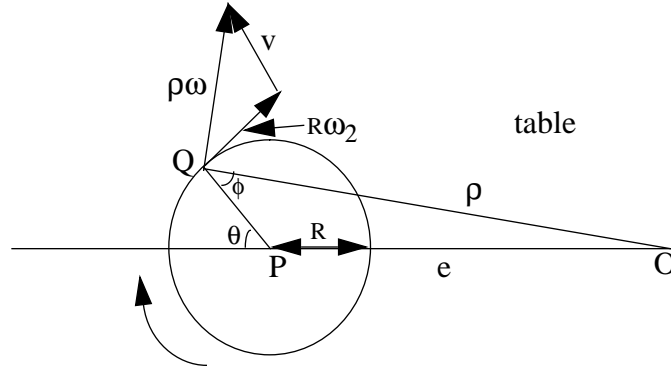


**Figure 1. Polishing machine setup detailing the velocity vectors of interest**

Let the angular rotation of the wafer and table be  $\omega_2$  and  $\omega$  (in radians per minute) respectively. Preston has obtained the relative velocity between pad and point  $Q$  of the wafer as:

$$v = v_s(1 + R_1^2\omega_s^2 + 2R_1\omega_s \cos\theta)^{1/2} \quad (2)$$

where  $v_s = e\omega$  is the relative velocity between any wafer position and pad if the wafer and pad are synchronized ( $\omega_2 = \omega$ ),  $R_1 = \frac{R}{e}$ , and  $\omega_s = 1 - \frac{\omega_2}{\omega}$ . Equation (2) may be reduced to:

$$v = v_s(1 + x^2 + 2x \cos\theta)^{1/2} \quad (3)$$

where  $x = R_1\omega_s$ . The effective relative velocity at any point at distance  $R$  from center is given by:

$$v_e(R) = \frac{v_s}{\pi} \int_0^\pi (1 + x^2 + 2x \cos\theta)^{\frac{1}{2}} d\theta \quad (4)$$

With the substitution  $\theta = 2\phi$  and  $\cos\theta = 1 - 2\sin^2\phi$ , the effective radial velocity becomes:

$$v_e(R) = \frac{v_s(1+x)}{\pi} \int_0^{\frac{\pi}{2}} \left(1 - \frac{4x}{(1+x)^2} \sin^2\phi\right)^{1/2} d\phi \quad (5)$$

which involves a complete elliptic integral of the second kind and is easily evaluated with standard computational packages such as Matlab™. Figure 2 shows typical variation of relative velocity from the center of the wafer for different carrier and table speeds. For typical machine settings,

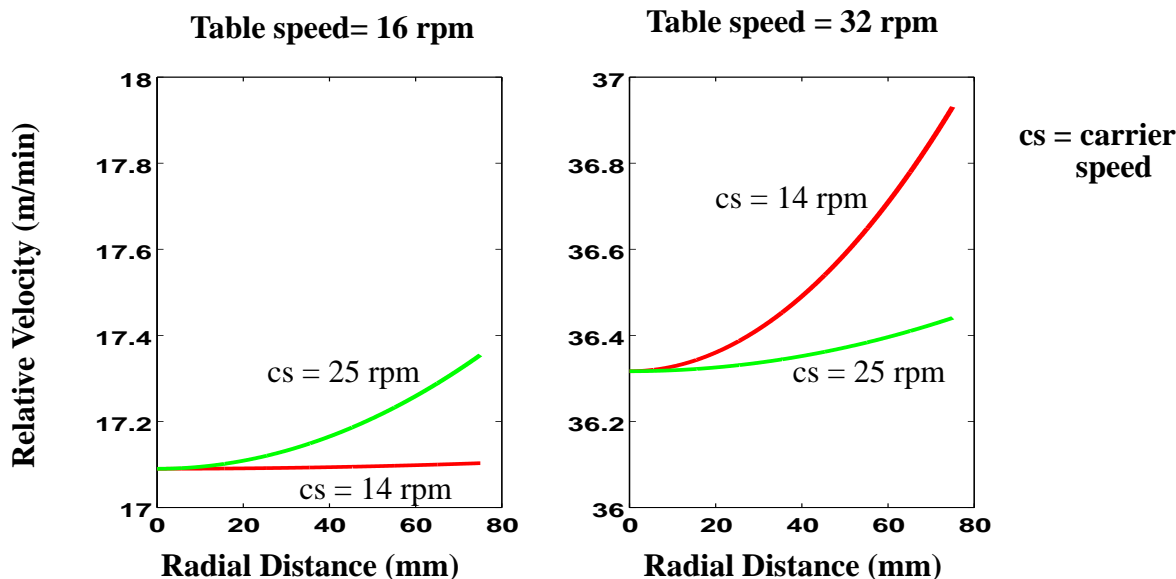


Figure 2. Relative velocity dependence on carrier and table speeds

center to edge variation is relatively small. For example, if the table angular velocity is twice the carrier angular velocity and the average carrier offset,  $e$ , is 170 mm, the percentage velocity change from center of the wafer to the edge is 1.2% for a 6" wafer and 2.2% for an 8" wafer. Center to edge variation in removal rate is usually much larger due to edge effect [5] which modifies the local pressure.

In typical polishing processes, there exist substantial wafer-level variation in removal rate. This may be due in part to the relative velocity variation but non-uniform pressure distribution arising from the carrier head design, and the edge effect are key contributors. Measurements reported in this paper were taken at 121 sites radially distributed on a 6" wafer but due to the strong edge effect, measurements taken beyond 55.2 mm radial distance are not used in model development. Figure 3 shows the effective radial removal rate obtained using an IPEC/Planar 372 polisher and an IC1400 polishing pad. The similarity of the profiles for different process conditions supports the assumption that a systematic source of variation exists.

### III. BLANKET POLISHING CHARACTERISTICS

In this section the results obtained from polishing blanket films are presented and we demonstrate the existence of two polishing regimes. Figure 4 shows results obtained from polishing blanket PETEOS films using two pads. Measurements were taken at the center of the wafers and the best fit to the experimental data is given by an equation of the form:

$$\frac{dz}{dt} = -[k_p p v + R_0]. \quad (6)$$

For PETEOS polishing,  $R_0$  is typically between 400 and 1000 Å/min. Obviously, when the product of pressure and velocity is zero, the removal rate is zero. To examine the polishing characteristics for low  $p v$ , experiments were performed with low down force and table speed. The minimum

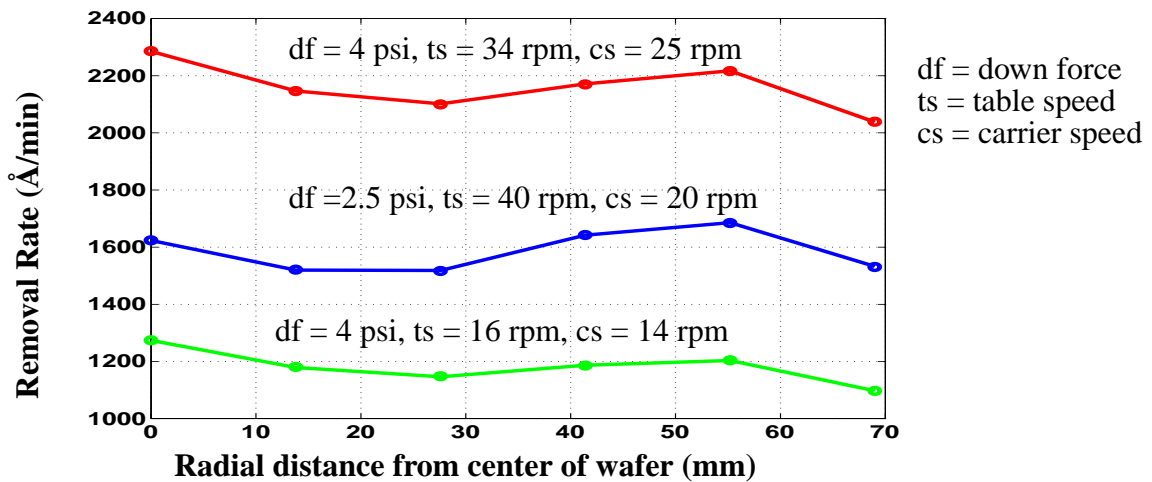


Figure 3. Typical wafer polishing profile for the machine used in this study

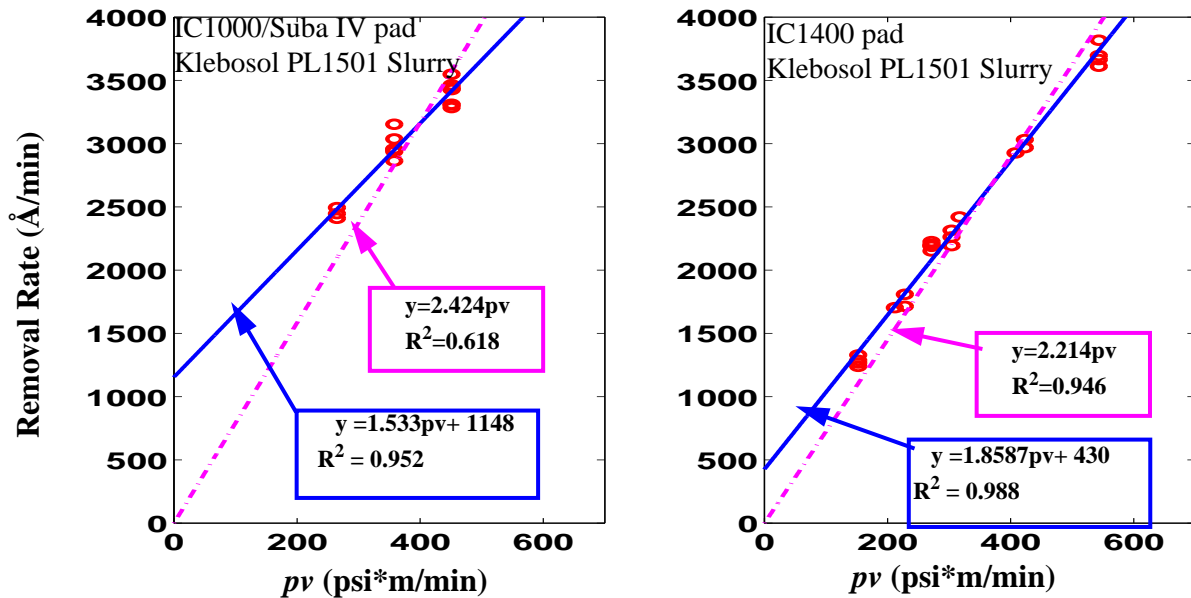
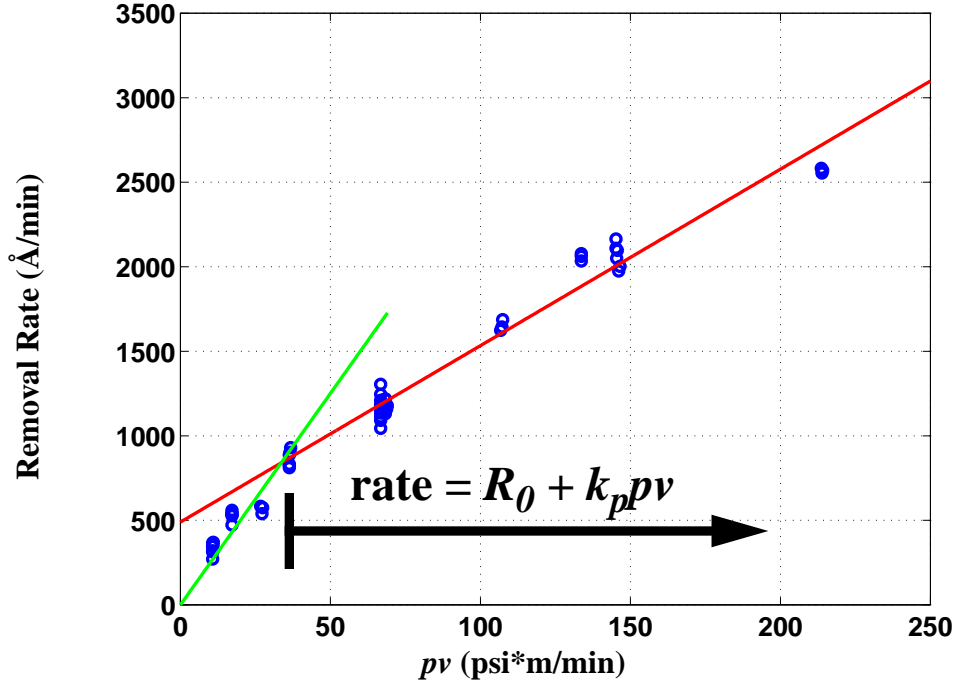


Figure 4. Blanket TEOS polishing rate results which demonstrate the need for inclusion of a constant term in Preston's equation.

table speed used was 10 rpm and the down force was reduced to 0.1 psi. The results are shown in Figure 5. Two regimes of operation are identifiable: for  $pv$  products above 50 ( $p$  in psi and  $v$  in m/min) the removal rate is linear in  $pv$  with an intercept,  $R_0$ , of approximately 500  $\text{\AA}/\text{min}$  which is consistent with the results obtained in Figure 4 for a similar pad. The scatter in the raw data is due to the systematic variation detailed in Section II. Below 50  $\text{psi}\cdot\text{m}/\text{min}$ , Preston's equation is satisfied with a large slope. This polish behavior may be explained by variation in polish efficiency; for very low  $pv$ , the polish efficiency is high since the supply of slurry to the wafer/pad interface is not impeded by high down force which squeezes the slurry out of the wafer/pad interface. The low table speed also minimizes slurry loss due to centrifugal action. The Preston equation is then satisfied with a large slope. As the  $pv$  increases, the polish efficiency is decreased. The combination of high down force and table speeds may result in less slurry at the wafer/pad interface, and the chemical component of polish is thus reduced. This effect is more pronounced at very high  $pv$



**Figure 5. Typical polishing characteristics for TEOS blankets showing what happens at low  $pv$ .**

where the removal rate is expected to flatten. The inclusion of a constant term has been proposed to account for chemical etching in metal CMP [6]. However, negligible material removal was observed when the TEOS wafers were immersed in slurry. In the next section we develop how the constant term may be incorporated into a pattern wafer polishing model to improve the model fit.

#### IV. MODIFICATION OF ILD THICKNESS MODEL

Stine et al. [3] have proposed a closed-form analytic model for ILD thickness for oxide CMP. The model is based on (1) which is reformulated as:

$$\frac{dz}{dt} = -\frac{K}{\rho(x, y, z)}. \quad (7)$$

$K$  is the blanket polish rate and  $\rho(x, y, z)$  is the local pattern density – defined as the ratio of “up” to total area within a square window centered at the point of interest. The window length is the planarization length of the polishing pad. The final ILD thickness is given by:

$$\begin{aligned} z &= z_0 - \left( \frac{Kt}{\rho_0(x, y)} \right) & Kt < \rho_0 z_1 & \quad (\text{nonlinear regime}) \\ z &= z_0 - z_1 - Kt + \rho_0(x, y)z_1 & Kt > \rho_0 z_1 & \quad (\text{linear regime}) \end{aligned}, \quad (8a)$$

$$\rho(x, y, z) = \begin{cases} \rho_0(x, y) & z > z_0 - z_1 \\ 1 & z < z_0 - z_1 \end{cases}. \quad (8b)$$

other variables are defined in Figure 6. As noted in the previous section, a constant term needs to

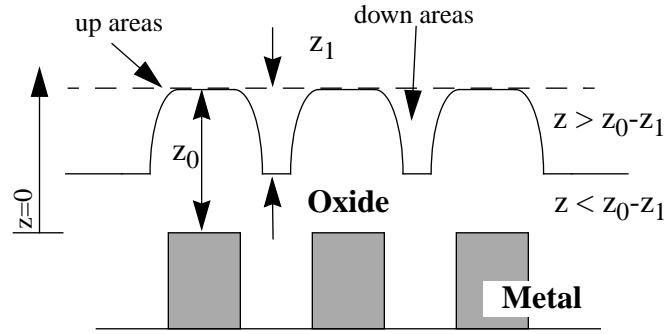


**Figure 6. Definition of terms used in model (after [6])**

be included in Preston's equation. Based on these results, (6) overestimates the pattern effect on film thickness: there is a constant offset in the Preston equation that should not scale with pattern density. The thickness relationship can be modified to:

$$z = z_0 - \left[ R_0 + \frac{K}{\rho_0(x, y)} \right] t \quad (9)$$

for the nonlinear regime ( $\rho_0 z_1 \geq (\rho_0 R_0 + K)t$ ) and to:

$$z = z_0 - z_1 - (R_0 + K)t + \left[ \frac{\rho_0 z_1}{\rho_0 R_0 + K} \right] [R_0 + K] \quad (10)$$

in the linear regime. Figure 7 shows a comparison of the model fit using (8) and (9-10). Values of  $R_0$  of 300 Å/min and 600 Å/min were used for IC1400 and IC1000/Suba IV polishing pads respectively. An improved model fit is obtained with the new model. This is more marked for very short polish times before complete local planarization of features (i.e. in the nonlinear regime). The  $R^2$  values are given for this regime.

## V. CONCLUSION

We have demonstrated the need for the inclusion of a constant term in Preston's model for blanket oxide wafer polishing. The modified equation has been incorporated into a pattern density-based analytic closed-form ILD thickness prediction for oxide CMP, and a better fit to experimental observation has been obtained.

## ACKNOWLEDGEMENTS

This work is supported in part by DARPA under contract #DABT63-95-C-0088 and by NSF/SRC Engineering Research Center for Environmentally Benign Semiconductor Manufacturing.

## REFERENCES

1. F. W. Preston, *J. Soc. Glass Technol.*, **11**, 247 (1927).
2. L. Cook, *J. Non-Cryst. Solids*, **120**, 152 (1990).
3. B. Stine et al., Proceedings of *CMP-MIC*, 266 (1997).
4. Y. Hayashide et al., Proceedings of *CMP-MIC*, 464(1995).
5. A. R. Baker, Proceedings of *Electro.. Chem. Soc. Meeting* **96-22**, 228(1996)
6. M. Weling et al., Proceedings of *CMP-MIC*, 65 (1997).

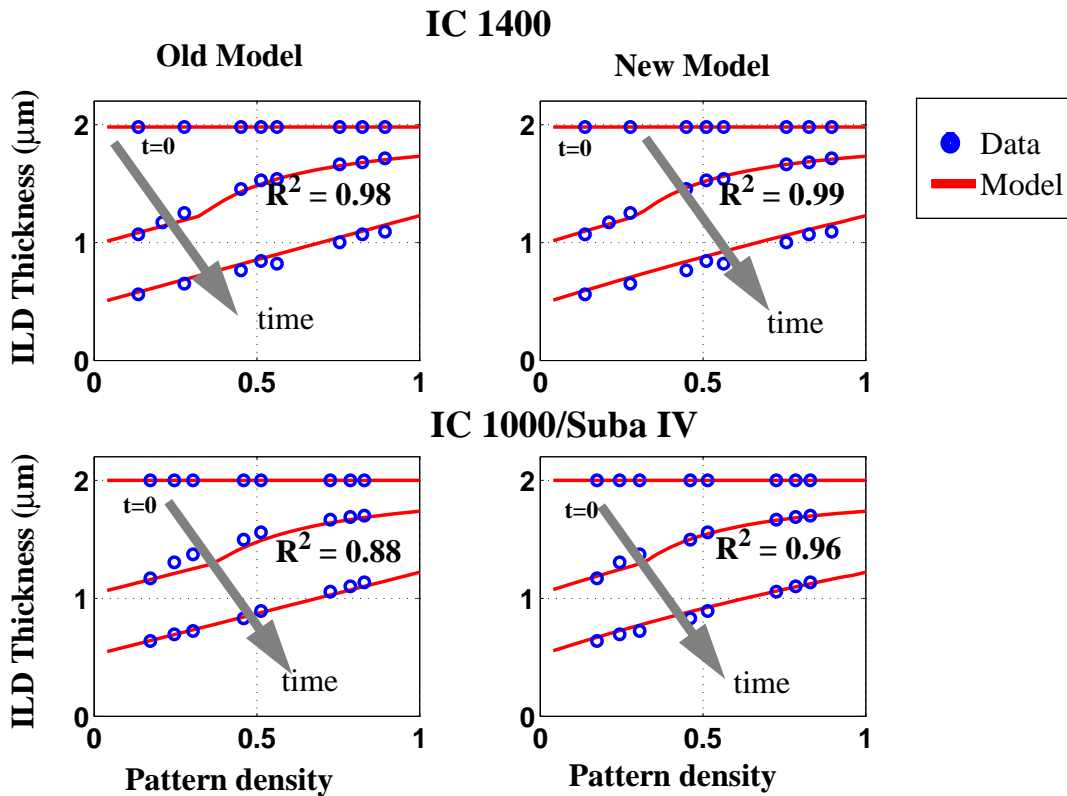


Figure 7. Comparison of old and new model.  $R_0$  is  $300 \text{ \AA}/\text{min}$  and  $600 \text{ \AA}/\text{min}$  for IC 1400 and IC 1000/ Suba IV respectively.